Downloaded from rsta.royalsocietypublishing.org

PHILOSOPHICAL TRANSACTIONS OF THE ROYAL SOCIETY A MATHEMATICAL, PHYSICAL & ENGINEERING SCIENCES

The Structure of a Weak Thermohaline Front [and Discussion]

P. J. Minnett, R. T. Pollard, D. S. Collins, A. Horch, M. Knoll, M. C. Gregg, J. D. Woods, S. A. Thorpe and M. G. Briscoe

Phil. Trans. R. Soc. Lond. A 1983 **308**, 359-375
doi: 10.1098/rsta.1983.0009

Email alerting service

Receive free email alerts when new articles cite this article - sign up in the box at the top right-hand corner of the article or click **here**

To subscribe to *Phil. Trans. R. Soc. Lond. A* go to: **http://rsta.royalsocietypublishing.org/subscriptions**

This journal is © 1983 The Royal Society

Downloaded from rsta.royalsocietypublishing.org

Phil. Trans. R. Soc. Lond. A **308**, 359–375 (1983)
Printed in Great Britain

The structure of a weak thermohaline front

By P. J. Minnett†§, R. T. Pollard‡, D. S. Collins‡, A. Horch† and M. Knoll†

† *Institut für Meereskunde, University of Kiel, F.R.G.*

‡ *Institute of Oceanographic Sciences, Brook Road, Wormley, Godalming, Surrey, GU8 5UB, U.K.*

A three-dimensional description of a near-surface thermohaline front is made possible by using data from a coordinated observational period (Second Multiship Experiment) in the Joint Air–Sea Interaction Experiment (JASIN 1978). The data are from current meters on buoys and high accuracy conductivity–temperature–depth probes used from fixed and mobile ships. The front is located in an eddy, which has length scales of order 100 km, and lies north–south marking the boundary of warm salty and cool fresh water masses. The thermoclinicity of the front is compressed into a narrow region often 500 m or less in width, and the vertical structure of thermoclinicity agrees remarkably well with the results of the numerical model of frontogenesis of MacVean & Woods (1980). The temperature and salinity structure are to a large extent mutually compensating in density with the result that the baroclinicity is too small to be convincingly detected in these data, which contain strong internal wave signals. Modulation of the static stability across the front is clearly seen and upwelling results in a drop of sea surface temperature of about 0.1 K above the front.

The front is advected through the observational array at about 0.75 km h^{-1} and, by using the current meter measurements, it is possible to use repeated sections across the front to investigate the along-front structure. Modulation of the thermoclinicity is observed resulting in local inversions, but extensive cross-frontal intrusions are not seen. The front appears to meander and the data are compared with the results of a numerical model of frontal instability (MacVean 1980).

1. Introduction

The three-dimensional structure of an upper ocean front encountered in the Joint Air–Sea Interaction Experiment, JASIN 1978 (Pollard *et al*, this symposium) is described in this paper. The data were taken in a coordinated intensive period of observations, designated the Second Multiship Experiment, which involved seven ships and two buoys, and permit an unusually detailed examination of the structure of the front. A great problem in investigating ocean fronts is the difficulty of making measurements on the whole range of pertinent scales, from those of eddies (order 100 km) to billows (order 10 cm). JASIN, however, provided a unique data set in which to frame this study, and the front described here should not be considered in isolation but in conjunction with the results of analyses of data on other scales from an eddy (Ellett *et al.* this symposium; Pollard 1982*a*) down to microstructure (Oakey 1982).

After a description of the Second Multiship Experiment, together with the instrumentation involved and the data reduction, in §2, the features of the front are examined in §3. The physical properties of the front are then assessed in §4 by comparing the observations with the results of numerical models. The frontogenesis model of MacVean & Woods (1980) successfully

§ Present address: Rutherford Appleton Laboratory, Chilton, Didcot, Oxfordshire OX11 0QX, U.K.

The Royal Society is collaborating with JSTOR to digitize, preserve, and extend access to *Philosophical Transactions of the Royal Society of London. Series A, Mathematical and Physical Sciences.* www.jstor.org

Downloaded from rsta.royalsocietypublishing.org

predicted some aspects of the thermoclinic structure, but the observed baroclinicity is weaker. The repeated sections enable us to describe the along-front variations. Meanders are resolved along the front (figure 8) and the thermoclinicity is strongly modulated with the spasmodic occurrence of inversions (figure 7). Comparison of the observed three-dimensional structure of the front with the results of the MacVean model of frontal instabilities (1980) is inconclusive.

2. The Second Multiship Experiment

The Second Multiship Experiment took place in the close vicinity of the H2 mooring (59° 25′ N, 12° 30′ W), some 47 km north of the Fixed Intensive Array (FIA) (59° N, 12° 30′ W) marking the centre of the JASIN area, on 2 and 3 September 1978 (days 245 and 246). Seven

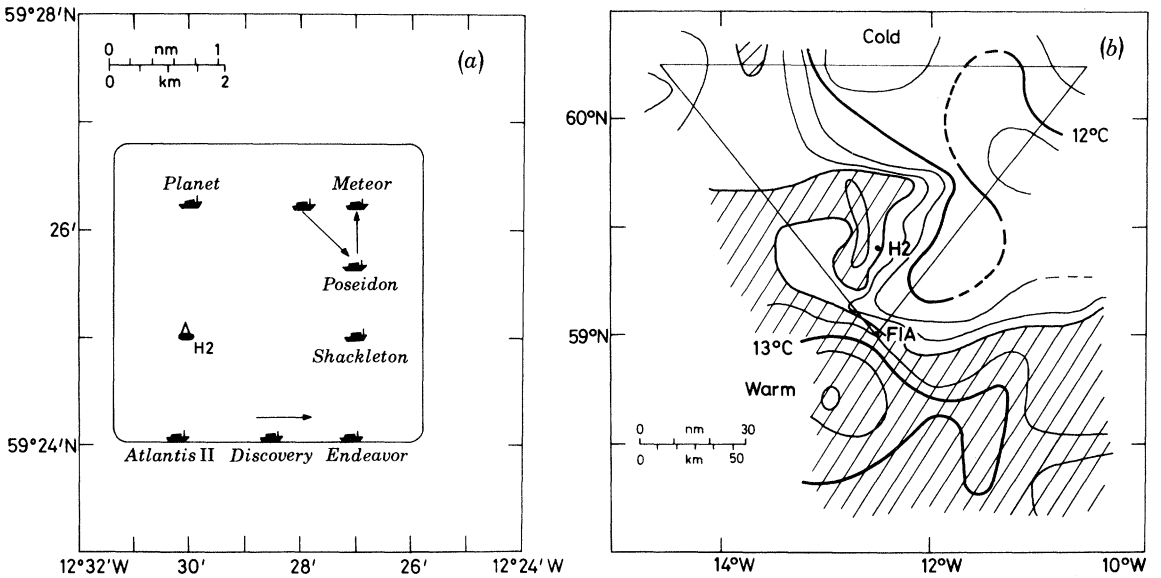

Figure 1. (*a*) A schema of the Second Multiship Experiment at the H2 mooring, from 10h00 G.M.T. on 2 September 1978 (day 245) to 15h00 on 3 September. The instrumentation is described in the text. The roving ships, R.V. *Endeavor*, R.R.S. *Discovery*, R.V. *Atlantis* II, sailed in line around the track shown at a speed of about 5.5 knots (2.8 m s^{-1}) taking a nominal two hours for each circuit, while synchronous conductivity–temperature–depth (CTD) profiles were made from the fixed ships at five-minute intervals.

(*b*) Mixed layer temperature (MLT) pattern in the JASIN area. The data cover the period from 27 August to 5 September, and show the surface manifestation of an anticyclonic eddy to the north of the Fixed Intensive Array (FIA), which lies at the southern apex of the meteorological triangle. The H2 mooring was about 47 km due north of the FIA. The shaded area shows MLT > 12.6 °C; the contour interval is 0.2 K. The data were compiled by Dr T. H. Guymer, from ship, mooring and aircraft measurements.

ships were involved: four holding station and three steaming in line around a square circuit enclosing the fixed ships and H2 (figure 1*a*). At the same time the P2 spar buoy, which had been released some 13 km northwest of H2 at the start of the Second Multiship Experiment, drifted southwards along a line about 10 km to the west of H2 (Pollard, this symposium).

The experiment began at 10h30 G.M.T. on 2 September (1030/245) with R.R.S. *Discovery* having already completed some circuits around H2 earlier that day before deploying P2. The ships remained committed to the joint activity until about midnight or later. R.R.S. *Discovery* continued to make circuits until after the H2 mooring was recovered at 1530/246 and remained in the area making circuits around P2 for a further three days (Pollard, this symposium). Throughout the period of the Second Multiship Experiment the wind was light.

Downloaded from rsta.royalsocietypublishing.org

A compilation of the mixed-layer temperature data (figure 1*b*) shows that the Second Multiship Experiment was situated south of the centre of an anticyclonic eddy (diameter about 85 km). This appears to have twisted the background meridional temperature gradient so that at H2 the larger-scale structure lies predominantly north–south.

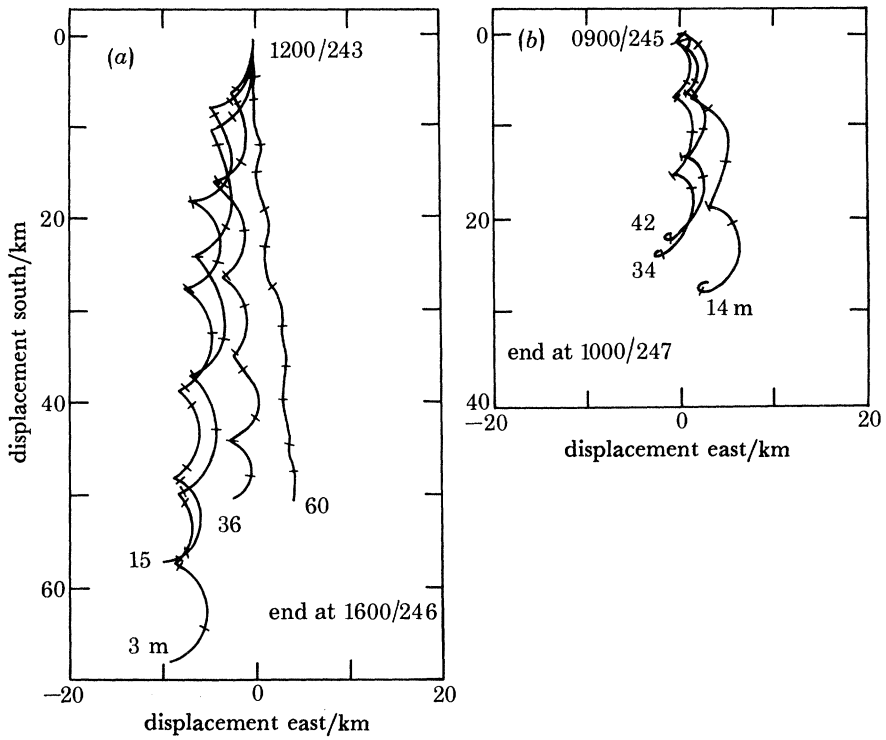

FIGURE 2. Progressive vector diagrams of the near-surface currents. The measurements are from current meters on (*a*) the H2 mooring and (*b*) the drifting spar buoy, P2, which was released 13 km northwest of H2 at the start of the Second Multiship Experiment (Pollard, this symposium) and proceeded to drift southwards. The measured P2 velocities have been made absolute (i.e. over-the-ground velocities) by using navigation data of the tending ship, R.R.S. *Discovery*, and fixes on the spar as described by Pollard (this symposium). The tick marks are at six-hour intervals, which include midnight. The traces show a mean southward flow with a superimposed tidal/inertial oscillation. In the 'mixed layer' the southward flow decreases slightly with depth while the amplitude of the oscillatory part is almost constant. Below the 'mixed layer' the oscillation has comparatively small amplitude.

Mooring instrumentation

The H2 mooring was a deep water (1700 m), taut-wire mooring with a toroidal surface buoy carrying a meteorological package and supporting current meters in the upper 60 m of the water column (Halpern 1979). At the time of the Second Multiship Experiment the current velocities were being measured by vector-averaging current meters (VACMS) (see, for example, Baker 1981) at 3, 15, 19, 36 and 60 m depth. Time series of temperature were also being measured at these depths and at 9, 25, 27 and 48 m. The instrumentation of the P2 spar buoy included current meters between 14 and 42 m depth, and is described by Pollard (this symposium).

Downloaded from rsta.royalsocietypublishing.org

Fixed ships' instrumentation and data reduction

From the start of the Second Multiship Experiment until the ships left the area, the fixed ships (R.V. *Meteor*, R.V. *Planet* and R.V. *Poseidon*) recorded profiles to 100 m starting in synchrony at five-minute intervals. The measurements were made with conductivity–temperature–depth probes (CTDs) lowered at 0.5 m s^{-1} in a 'yoyo' fashion. A Neil Brown Instrument Systems' (N.B.I.S.) CTD (Brown 1974) was used from R.V. *Poseidon* and ME Multisondes (Kroebel 1973) were in use from R.V. *Meteor* and R.V. *Planet*.

The raw data consisted of measurements of temperature, conductivity and pressure with high vertical resolution (less than 10 cm), from which salinity and density were calculated after calibration and correction of corrupt data points (including time-constant corrections). The profiles were then made monotonic to remove the effect of ship roll, smoothed with a 0.5 dbar† running filter and resampled at 0.5 dbar in pressure and 0.005 kg m^{-3} in density (σ_T). The data reduction is described in more detail elsewhere (Horch *et al.* 1982).

The accuracies of temperature and pressure are better than ± 0.01 K and ± 1.0 dbar, with uncertainties in derived salinity and density (σ_T) of about ± 0.01‰ and ± 0.01 kg m^{-3}. In regions of sudden changes in the temperature gradient, local degradation to about twice these values in temperature, salinity and density may occur, but even these are too small to mask the clear frontal signal.

The CTD profiles made by R.R.S. *Shackleton* were interspersed with measurements of the temperature and velocity microstructure (Oakey 1982).

Roving ships' instrumentation and data reduction

The ships steamed around the square circuits shown diagrammatically in figure 1*a* at about 5.5 knots (2.8 m s^{-1}) in the sequence shown. The sides of the square were about 5 km long and the circuits each took about two hours to complete.

R.V. *Endeavor* was equipped with an acoustic profiler and R.V. *Atlantis* II towed a thermistor chain (Baumann *et al.* 1980), for both of which the dominant signal came from internal waves. In §3 it will be shown that the front was strongly thermoclinic, requiring the measurement of conductivity (to derive salinity and density) to reveal its structure. For this reason the emphasis on roving-ship data is given here to those taken from R.R.S. *Discovery*, which towed a Neil Brown Instrument Systems' CTD in an Institute of Oceanographic Sciences' Sea-Soar. The Sea-Soar is a development of the Canadian Batfish (Dessureault 1976), being a towed vehicle with active hydroplanes, which are tilted on command from a controller on board the parent vessel. Two sawtooth patterns were used on alternate circuits: an asymmetrical form with slow ascents and a symmetrical form with both ascents and descents at about 1.0 m s^{-1} (inclination of the Sea-Soar track is then about 20°). The Sea-Soar data presented here are taken only from the alternate circuits with the symmetrical waveform, which gives much better horizontal sampling of the front throughout the whole depth range, numbered 125 to 143 (odd numbers only). The start time of each circuit is shown in table 1. The P2 buoy was launched between circuits 127 and 129.

In situ calibration of the Sea-Soar CTD is difficult. These circuits, in which water with the same temperature, salinity (T, S) characteristics was repeatedly sampled, provided a useful framework in which to establish internal consistency in the data set (Pollard 1980). Absolute

† 1 bar = 10^5 Pa.

PHILOSOPHICAL TRANSACTIONS OF THE ROYAL SOCIETY A MATHEMATICAL, PHYSICAL & ENGINEERING SCIENCES

PHILOSOPHICAL TRANSACTIONS OF THE ROYAL SOCIETY A MATHEMATICAL, PHYSICAL & ENGINEERING SCIENCES

Downloaded from rsta.royalsocietypublishing.org

calibration is achieved by comparison with T, S relations measured at nearby ships. The residual salinity errors are in general smaller than 0.02‰, and the accuracy of the temperature measurements is 0.01 K (Pollard, this symposium). The T, S relations measured by R.R.S. *Discovery* and the fixed ships show good agreement, to the level imposed by oceanic variability. For our purposes averaged values over 1 dbar of the Sea-Soar CTD data were derived for the descending parts of each sawtooth.

TABLE 1. START TIMES OF SEA-SOAR CIRCUITS AROUND H2 (SECOND MULTISHIP EXPERIMENT)

circuit number	start time (time/day)	circuit number	start time (time/day)
125	0000/245	135	2232/245
127	0346/245	137	0240/246
129	1023/245	139	0701/246
131	1413/245	141	1103/246
133	1826/245	143	1515/246

Navigation and relative positions

Throughout the period of the Second Multiship Experiment the position of R.R.S. *Discovery* was monitored every half hour using Loran C, which was found to give better fixes (r.m.s. error $\approx$ 200 m) than the satellite navigation (Pollard, this symposium). The measurements of the ship's electromagnetic log were used to interpolate the ship's track between the Loran fixes, giving the geographical position of the ship (see figure 9 of Pollard & Saunders (1978)).

While the roving ships made the repeated circuits, the southward ocean currents (figure 2) advected the water through the H2 area, resulting in different water being sampled at each repeated section. To represent the 'spatial' extent of the measurements, relative coordinates were devised making use of the time series of currents measured at H2. Choosing an arbitrary time origin (2230/244, when R.R.S. *Discovery* began the Sea-Soar circuits) the absolute ship's position has been displaced by the time integral of the current measured at 15 m depth. The resulting relative positions are given as distance north and east of the FIA (see figure 6) and, by invoking Taylor's hypothesis, the measurements could be interpreted as synoptic observations of the frontal structure at 2230/244 at the relative positions shown.

The fixed ships also took navigation fixes at frequent intervals (15 or 30 min) with Loran C and Decca Navigator. Furthermore, radar fixes on each ship and H2 were made. A thorough analysis of the data has been made and the deviations from the mean station positions were found to be generally less than 500 m. The positions of R.V. *Meteor* and R.V. *Planet* have also been transformed into relative coordinates by the same technique as above and these are also shown in figure 6.

3. DESCRIPTION OF THE FRONT

The accurate navigation data for each ship locate the measurements in geographical coordinates but, even after transformation of the data into relative coordinates, it is necessary to understand the larger-scale current field, which advects the features through the measurement grid. The currents measured at H2 for a period that includes the Second Multiship Experiment are shown in figure 2*a* as progressive vector diagrams. The predominant flow is to the south (about 0.75 km h^{-1} at 15 m depth) with a superimposed oscillation with tidal (12.4 h) or

PHILOSOPHICAL TRANSACTIONS OF THE ROYAL SOCIETY A MATHEMATICAL, PHYSICAL & ENGINEERING SCIENCES

PHILOSOPHICAL TRANSACTIONS OF THE ROYAL SOCIETY A MATHEMATICAL, PHYSICAL & ENGINEERING SCIENCES

Downloaded from rsta.royalsocietypublishing.org

inertial (13.8 h) period. The amplitude of the oscillation is such that the zonal excursion of a water particle is about 3 km.

The effect of shears in the water column is to displace particles of water with respect to those at the reference level of 15 m, which can introduce distortions into the representation of the data as sections (figures 5 and 7). The mean shears from the measurements at H2 are shown in table 2 for the period including the Second Multiship Experiment. Variability in the shears can lead to larger displacements over intervals smaller than the tidal period and, to illustrate this, the values for the six-hour period shown in figure 5 are included in table 2 (bracketed).

TABLE 2. MEAN SHEAR IN H2 CURRENTS FOR PERIODS 1200/243 TO 1600/246 (AND 1430/245 TO 2030/245)

depth interval/m	mean shear 10^{-3} s^{-1}	displacement speed/(m h^{-1})	heading/deg
3–15	3.2 (6.2)	138 (269)	180 (300)
36–15	1.5 (5.0)	122 (382)	50 (300)
60–15	1.2 (0.24)	200 (40)	65 (350)

These values are of course at H2 and are not measured at the front nor at the places the ships' measurements were made. For comparison the current measured at P2, some 10 km to the west, is shown in figure 2*b*. Further, it will be shown below that the front has quite small baroclinicity and so has correspondingly small shear across it. Examination of the R.R.S. *Discovery* navigation data reveals no measurable difference in the southward advection between the eastern and western sides of each circuit. Consequently it is believed that the currents measured at H2 are reasonably representative of those in the area of the Second Multiship Experiment. The distorting effects of the shear on the sections shown later should, however, be borne in mind when the figures are examined.

T, S variability

As can be seen from figure 1*b*, the front separates warmer water of southern origin from cooler water, the background gradients having been contorted by the effect of an eddy. The change in the *T, S* properties across the front is shown in figure 3. Five profiles are shown in each panel: (*a*) R.V. *Planet* from 2030 to 2130/245, (*b*) R.V. *Meteor* from 1730 to 1930/245 and (*c*) R.V. *Meteor* from 1430 to 1530/245. The water on the eastern side of the front (figure 3*c*) is cooler and less saline near the surface than that to the west. The changes in temperature and salinity at $\sigma_T = 26.60$ kg m^{-3} are 0.32 K and 0.077‰. Below $\sigma_T = 26.76$ kg m^{-3}, the difference between the water masses is smaller, becoming negligible at about $\sigma_T = 27.15$ kg m^{-3}. Warmer, saltier intrusions appear, however, at $\sigma_T = 27.23$ kg m^{-3} and about 27.28 kg m^{-3} at the western station.

Baroclinicity

The change in the thermohaline properties of the water across a front can, and often does, lead to a change in the density field. The horizontal pressure gradients resulting from the density structure are then associated with a velocity shear, which in the simplest case and assuming geostrophy, is described by Margules equation (see, for example, Stern 1975, p. 72).

Downloaded from rsta.royalsocietypublishing.org

Figure 4 shows typical sections across the front and includes the density (σ_T) structure in pressure coordinates. The largest signal appears to be due to internal waves. The horizontal temperature gradient in the surface layer, marked by near vertical isotherms (figure 4*a*), is almost entirely compensated by a similar salinity gradient, with the consequence that the front has only a slight signature in the density field. When the fields are smoothed horizontally with an equivalent 1 km filter, a trend in the density at a given depth is revealed (the 40 dbar isobar is shown in figures 4*c*, *d*). The geostrophic velocity calculated from the smoothed density field shows two subsurface 'jets' at a depth of 30 m, with maximum horizontal shear of about 3 cm s^{-1} across 1.8 km. These are associated with the upwelled tongue of cool dense water (figures 4*a*, *b*), while the shear due to the front itself is not resolved in the data.

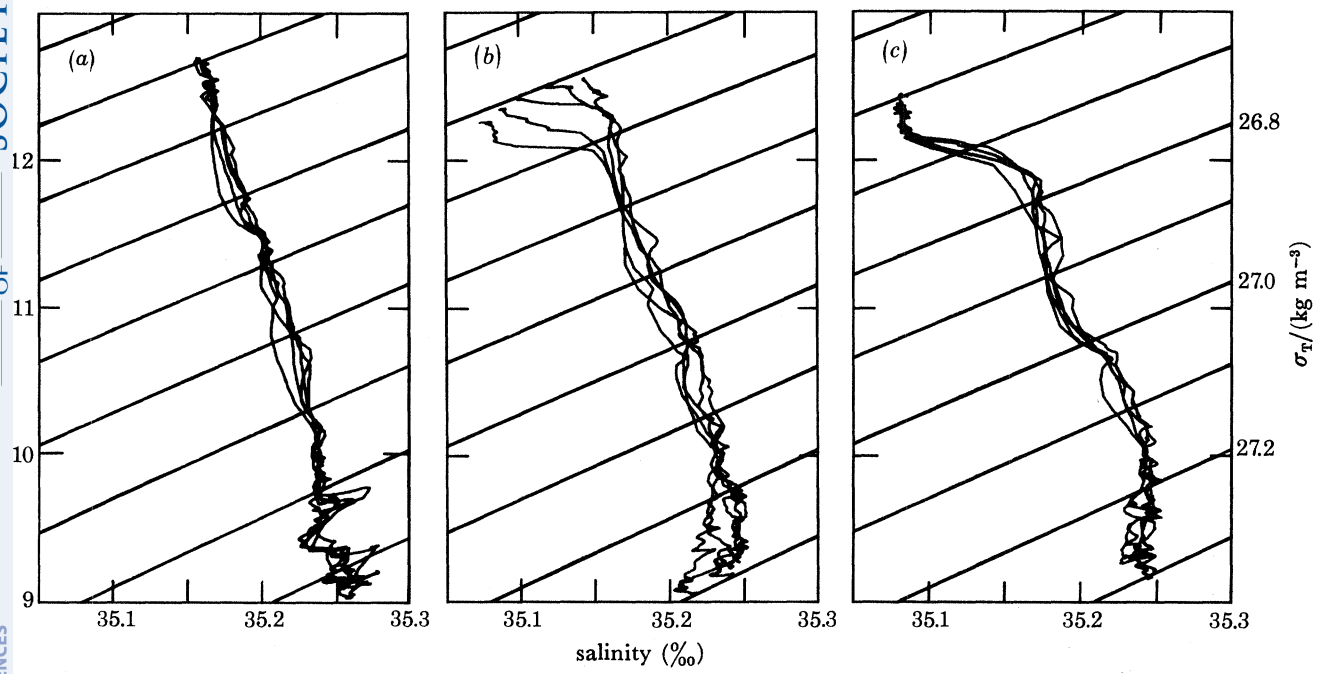

FIGURE 3. The change in the *T*, *S* relation is shown in 100 m CTD profiles from (*a*) R.V. *Planet* and (*b*), (*c*) R.V. *Meteor*. Two panels contain five profiles at 15 min intervals, showing (*a*) 'western water', (*c*) 'eastern water', and part of the transition across the front (*b*) is shown with profiles at 30 minute intervals.

The sections of density (σ_T) as a function of pressure drawn from the data of R.V. *Planet* and R.V. *Meteor* (figures 5*a*, *d*) show also the dominance of the internal wave signal. However, the vertically coherent part, due to internal waves of low vertical mode, can be removed by referring the pressure at any isopycnal to that on a reference isopycnal (arbitrarily chosen). The result, figures 5*c*, *f*, is clearest for R.V. *Planet*, showing a general convergence of the isopycnals to the east. This can be discerned in figure 5*a*.

Returning now to the Sea-Soar sections, the same procedure can be followed to remove much of the internal wave signal. As the Sea-Soar did not consistently penetrate the σ_T = 27.0 kg m^{-3} isopycnal, the reference level of σ_T = 26.70 kg m^{-3} was chosen (figure 8*b*). The pressure difference between σ_T = 26.66 kg m^{-3} and the reference level is shown as contours in relative coordinates north and east. A tongue of large separation of the isopycnals (low static stability) is seen to extend northwards. As the time interval involved (0030/245 to

PHILOSOPHICAL TRANSACTIONS OF THE ROYAL SOCIETY A MATHEMATICAL, PHYSICAL & ENGINEERING SCIENCES

Downloaded from rsta.royalsocietypublishing.org

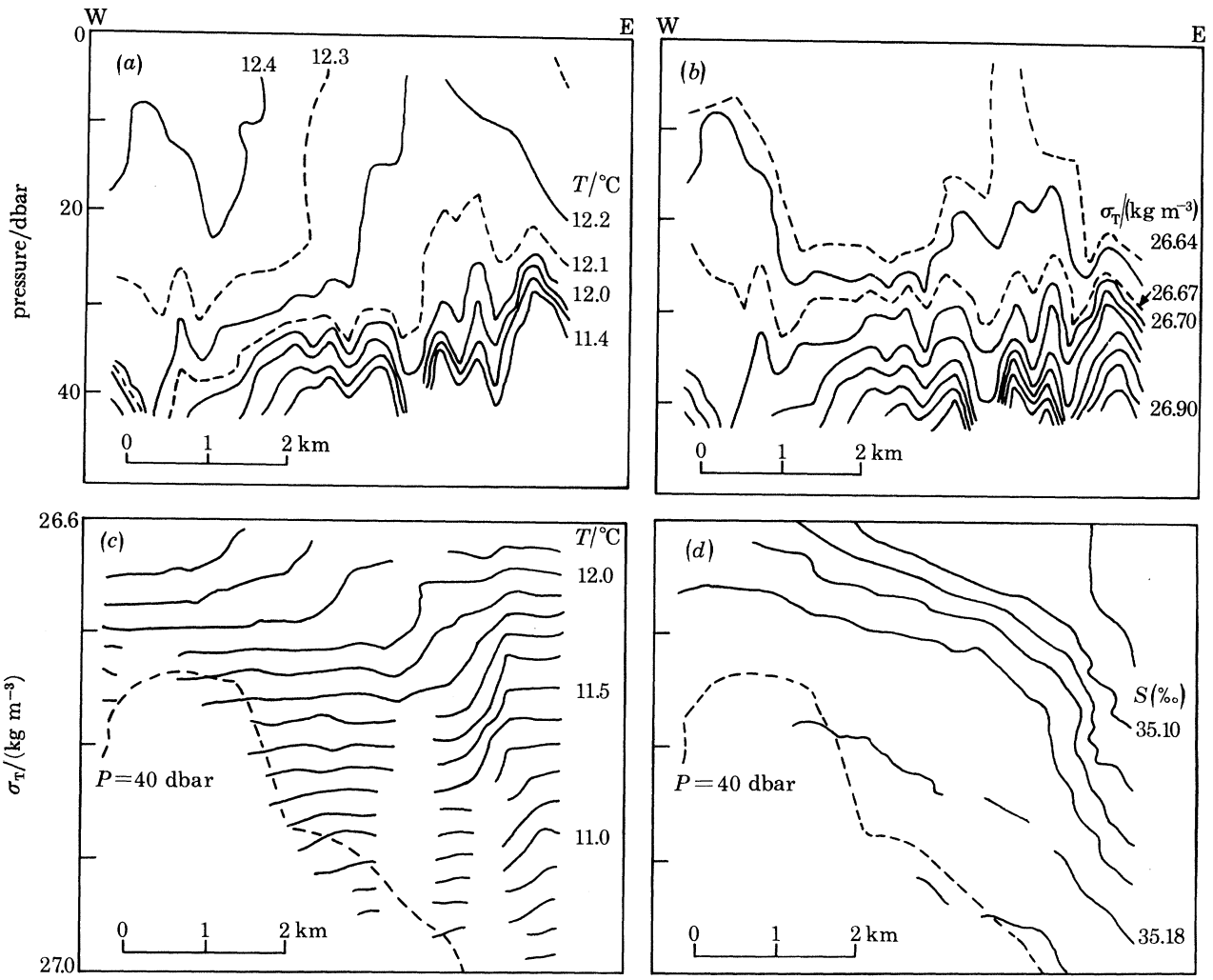

FIGURE 4. A typical section across the front. The data are from the north side of circuit 131, positioned at 61 km north of the FIA in relative coordinates (see figure 3 and text). The section, from 1510 to 1535/245, is about 5.3 km in length, took about half an hour and contains 24 Sea-Soar cycles. The diagrams show (*a*) temperature as a function of pressure, with full contours at $\delta T = 0.2$ K; (*b*) density (σ_T) as a function of pressure, with full contours at $\delta\sigma_T = 0.05$ kg m^{-3}; (*c*) temperature as a function of density, $\delta T = 0.1$ K; (*d*) salinity as a function of density, $\delta S = 0.02$‰. In (*c*) and (*d*) the position of the (smoothed) 40 dbar isobar, which is close to the bottom of the Sea-Soar depth range, is shown.

1530/246) encompasses several inertial cycles, it is unlikely that the signal is of internal wave or tidal origin.

Thermoclinicity

The term 'thermoclinicity' (and similarly 'haloclinicity') can be used to describe the inclination of isotherms (or isohalines) in density space just as baroclinicity describes the inclination of isobars (Defant 1961, vol. 1, p. 308). In regions where there are changes in the T, S relation, such as at fronts, the thermoclinicity has a local maximum.

While the baroclinic signal at the front is very weak the thermoclinicity, and consequently the haloclinicity, show strong signals (figures 4*c*, *d*). For instance, the density at which the 11.6 °C isotherm is found changes from $\sigma_T = 26.716$ to $\sigma_T = 26.794$ kg m^{-3} in a horizontal distance

Downloaded from rsta.royalsocietypublishing.org

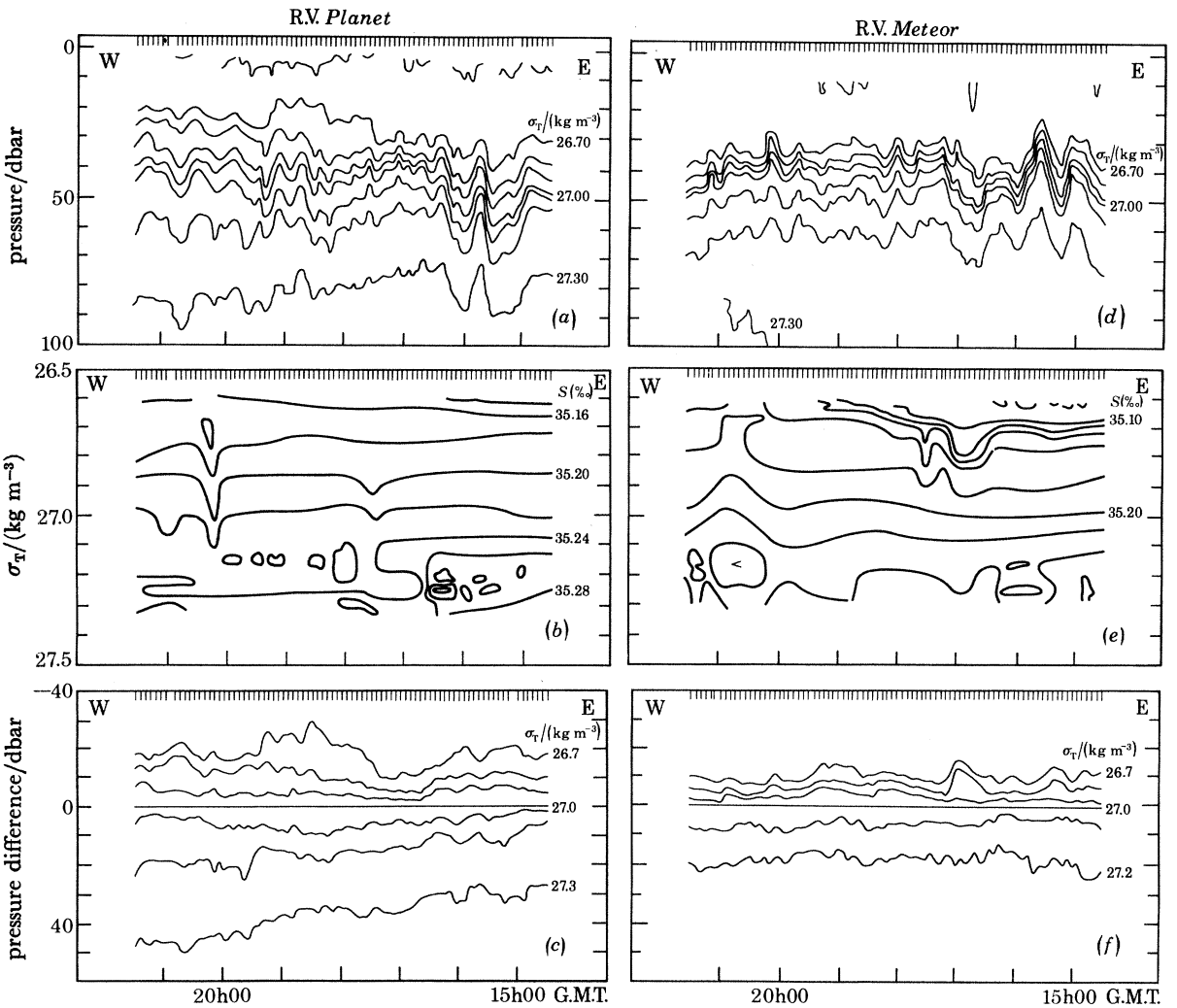

FIGURE 5. 100 m CTD profiles from the fixed ships show the frontal structure extending below the 40 m depth range of the Sea-Soar. The time series of profiles shown here are from R.V. *Planet*, (*a*)–(*c*), and R.V. *Meteor*, (*d*)–(*f*), taken at five minute intervals from 14h30 to 20h30 G.M.T. on 2 September. The tick-marks at the top border indicate the start-times of the profiles; only the descending parts have been used here. The effect of advection is to reveal cross-frontal structure. These diagrams correspond to a single section through the front. The relative positions of the ships' stations are shown in figure 6.

(*a*) and (*d*) Density, σ_T, against pressure. The front does not have strong baroclinicity and internal waves contribute the largest signal.

(*b*) and (*e*) Salinity against density, σ_T. The strong haloclinicity at the front is revealed. The shallower signal at the eastern station (R.V. *Meteor*) is stronger than to the west, where a strong deeper signal can be seen.

(*c*) and (*f*) The effect of internal waves with high vertical coherence can be removed by reducing the pressure at isopycnals by that on an (arbitrary) reference isopycnal (σ_T = 26.70 kg m^{-3}). The change in static stability across the front is most obvious in the R.V. *Planet* data, and appears on a much longer 'length' scale than the haloclinic signal.

PHILOSOPHICAL TRANSACTIONS OF THE ROYAL SOCIETY A MATHEMATICAL, PHYSICAL & ENGINEERING SCIENCES
PHILOSOPHICAL TRANSACTIONS OF THE ROYAL SOCIETY A MATHEMATICAL, PHYSICAL & ENGINEERING SCIENCES

Downloaded from rsta.royalsocietypublishing.org

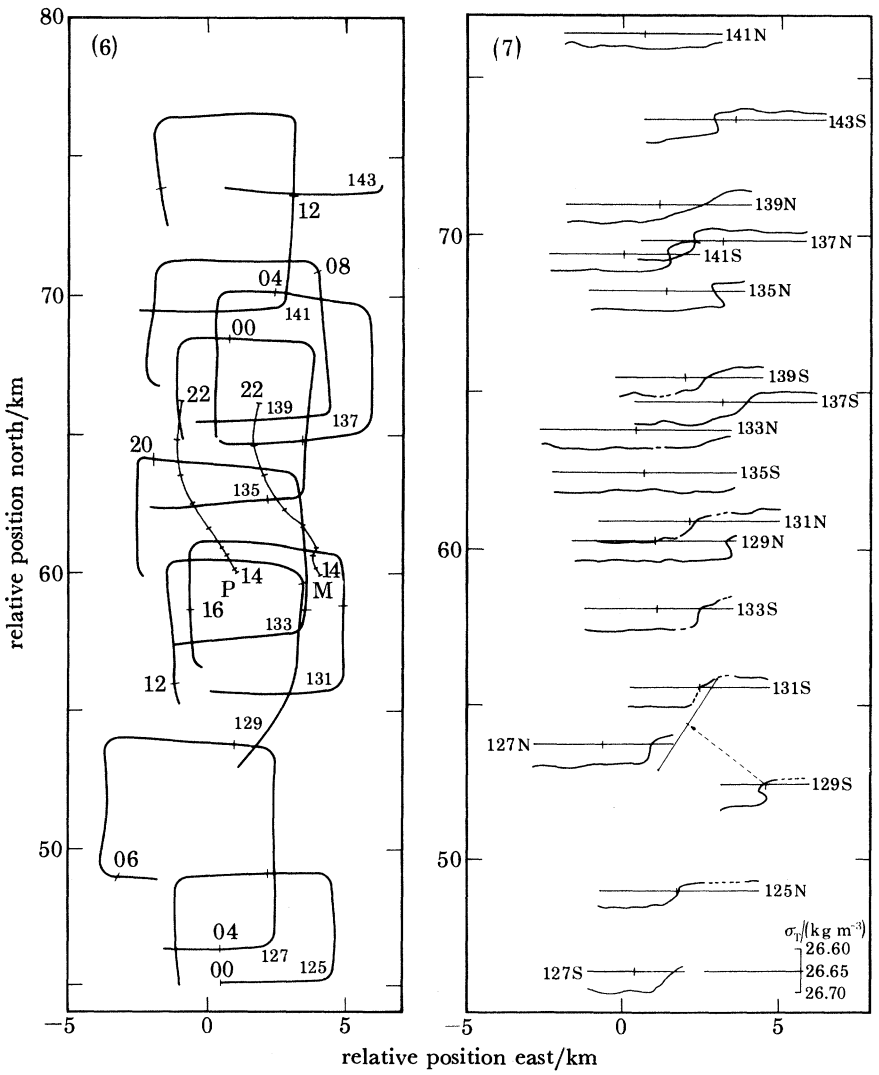

FIGURE 6. The positions of the fixed ships R.V. *Meteor* (M) and R.V. *Planet* (P) and of the Sea-Soar circuits of R.R.S. *Discovery* are shown in relative coordinates, which have origin at the FIA at 2230/244. The effect of the current is to advect the frontal structure under the ships' positions (see text). The fixed ships' positions are for the period 1400–2200/245, corresponding to that shown in figure 5, with hourly tick-marks. The number of each Sea-Soar circuit is shown and tick-marks again correspond to one-hour intervals.

FIGURE 7. Repeated Sea-Soar sections through the front reveal variations along the front as it is advected by the southward flow. Here the 12.1 °C isotherm is plotted in σ_T coordinates and shows the changing thermoclinicity. The scale at bottom right gives the vertical, σ_T, scale for each section. The thin line associated with each isotherm marks the 26.65 kg m^{-3} isopycnal level and is positioned at the location of the section in the relative coordinates centred at the FIA (see figure 6 and text). Each section is identified by the circuit number and N or S, to denote north or south side. The periodic appearance of temperature inversions is not obviously connected with the east–west displacement of the section, which is caused by the tidal/inertial oscillation advecting the front under the geographically fixed location of circuits.

Downloaded from rsta.royalsocietypublishing.org

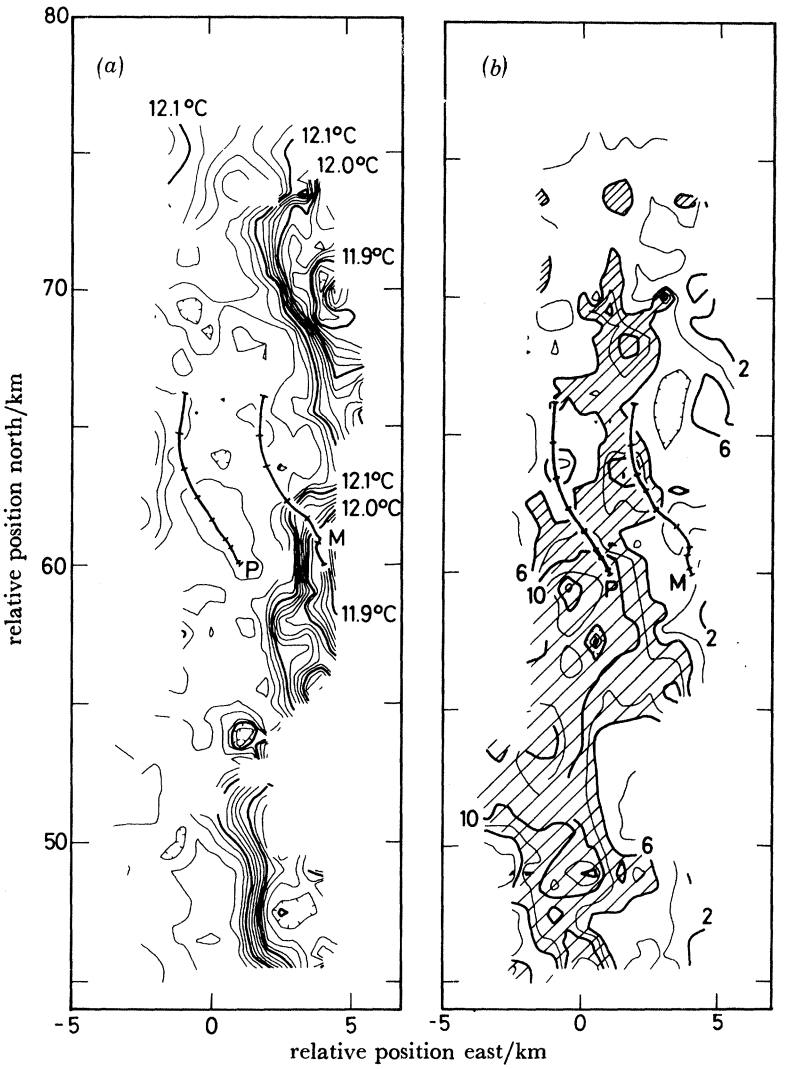

FIGURE 8. (*a*) The temperature measured by the Sea-Soar at the density $\sigma_T = 26.70$ kg m^{-3}. The region of large thermoclinicity is easily identified to the east. The positions of R.V. *Meteor* (M) and R.V. *Planet* (P) are shown to allow comparison with figure 5. Closed contours marked with ticks encircle a local minimum.

(*b*) The pressure difference (in dbar) between the density surfaces $\sigma_T = 26.66$ kg m^{-3} and $\sigma_T = 26.70$ kg m^{-3} as measured by the Sea-Soar. Small values indicate high static stability. A tongue of low static stability ($\delta P > 6$ dbar) is shaded and lies to the west of the position of maximum thermoclinicity. Again the positions of R.V. *Meteor* (M) and R.V. *Planet* (P) are shown.

of 0.57 km. Towards lower densities the locus of the thermoclinicity maximum becomes much less inclined, even though the value of the local thermoclinicity maximum remains high; indeed local inversions occur. Away from this narrow region of the thermoclinicity maximum, the thermoclinicity rapidly decreases.

The haloclinicity observed from R.V. *Meteor* and R.V. *Planet* is shown in figures 5*b*, *e*. The shallow signal is well resolved in the *Meteor* data, but is missing in the *Planet* data, indicating that the strongest part of the thermoclinic front was not advected as far west as *Planet's* station. Deeper in the pycnocline, however, strong haloclinicity was found and at this level in the

Downloaded from rsta.royalsocietypublishing.org

Meteor data the signal is confused. These structures are presumably associated with instrusions as seen in the T, S diagrams (figure 3*a*).

Along-front variations

By comparing the repeated traverses across the front it is clear that the cross section is quite variable. This is shown in figure 7 where the shape of the 12.1 °C isotherm, in σ_T coordinates, is shown for each north and south side of the circuits. The southern side of circuit 129 was taken on a northeasterly heading as R.R.S. *Discovery* returned from deploying P2 and lay along the line shown.

The zonal displacement of the reference $\sigma_T = 26.65$ kg m^{-3} isopycnal (thin lines in figure 7) is due to the advection by the tidal/inertial currents. Variation of the position of maximum thermoclinicity in the relative coordinate frame indicates either meanders on the front or that current shear, vertical or horizontal, between the 15 m current meter at H2 and this isotherm at the front invalidates the method of deriving relative positions. The mean depth of the 12.0 °C isotherm at H2 (from 2230/244 to 1530/246) was 28.9 dbar.

To explain the amplitude of the zonal displacement of the position of maximum thermoclinicity, about 2 km, in terms of vertical shear between 15 and 29 m depth, a shear of 1.8 s^{-1} with an inertial period would be needed; this is several orders of magnitude larger than those observed. For the signal to have been caused by horizontal shear in the internal tide, the tide at H2 and at the front would have had to have been in near antiphase, as the amplitude of the tidal/inertial signal is about half that of the frontal displacement. As the maximum separation between H2 and the Sea-Soar circuits was 6 km, this can hardly have been so. Thus the measured displacement of the front, when shown in relative coordinates, must be environmental.

The meandering nature of the front is well revealed when isotherms on an isopycnal are plotted in relative coordinates (figure 8*a*). The position of maximum thermoclinicity lying to the eastern side of the Sea-Soar survey is well delineated and has a wavelike form with wavelength about 12 or 25 km.

4. Discussion

The Sea-Soar sections show that the thermoclinicity at the front is compressed into a very narrow band, often less than 0.5 km wide. This width changes in successive crossings and appears to be modulated along the length of the front, frequently giving rise to inversions. The modulation of the width of the thermoclinic band may result entirely from the Sea-Soar section's intersecting the front at different angles (satellite images have shown just how convoluted the surface outcrops of fronts can be; see for example Legekis (1978)), and the apparent horizontal extent of the inversions can also be altered by changing the angle between the section and the axis of the thermoclinic band. The consequence of a shallow angle between section and front is an exaggerated intrusion at an inversion (which may be the case in 129S, figure 7) and an increased width of the thermoclinic band. This effect alone, however, cannot introduce inversions where none occur. Vertical shear in the inertial wave, on the other hand, could cause inversions. However, this is unlikely to have been the cause as sections 137N and 141S (figure 7) are separated by about half an inertial period, yet both show an inversion. One must conclude that the observed inversions are a property of the front itself.

Comparison with the results of a numerical model of frontogenesis (MacVean & Woods

PHILOSOPHICAL TRANSACTIONS OF THE ROYAL SOCIETY A MATHEMATICAL, PHYSICAL & ENGINEERING SCIENCES

PHILOSOPHICAL TRANSACTIONS OF THE ROYAL SOCIETY A MATHEMATICAL, PHYSICAL & ENGINEERING SCIENCES

Downloaded from rsta.royalsocietypublishing.org

1980) does, however, confirm that much of the thermoclinic structure in individual sections is attributable to the front. Many similarities are to be seen, for instance, between figure 4*c* of this paper and figure 9 of MacVean & Woods (which is plotted in depth rather than density coordinates, but which, owing to the smoothness of the model isopycnals, can be easily envisaged in σ_T coordinates), including the increase in the width of the thermoclinic band with depth while the axis of the maximum thermoclinicity becomes steeper. Furthermore, inversions of the same appearance as those in the Sea-Soar sections are produced close to the surface in the model. The ratio of the length scales of the baroclinic and thermoclinic fields in the fully developed model front varies from about 0.1 close to the surface to about 0.03 deeper (12.5 and 87.5 m respectively). If the conditions at the Second Multiship Experiment front are reflected by those in the numerical model, then the width of the baroclinic band associated with the observed thermoclinic signal would be in excess of 5 km and thus not defined in the length of the Sea-Soar sections. A major difference between the observations and the model results is that the horizontal velocity shear associated with the frontal jet in the model has a maximum of about 6 cm s^{-1} km^{-1} at the surface, and a signal of this size would have been seen in the geostrophic velocities derived from the measurements. Consequently we must conclude that the salinity and temperature changes across the front compensate each other in the density field to a larger degree in the observations than in the model.

The inclination of the axis of maximum baroclinicity results, in the model, in a modulation of the pressure difference between adjacent isopycnals across the front, there being a local minimum next to a local maximum in static stability. The position of the increased separation between isopycnals is displaced to the warm side of the position of maximum thermoclinicity. This signature is sufficiently strong, even in the weak observed baroclinicity, that it can be seen above the level of the internal wave signal and it does indeed lie about 1–3 km to the warm side of the position of maximum thermoclinicity (figure 8). A similar, but much weaker, signal was observed in the tropical thermocline during the GARP Atlantic Tropical Experiment (GATE) (Minnett 1978), also in a region where the internal waves masked the baroclinicity associated with observed thermoclinicity.

Many other reports of observations at fronts have described tongues of water crossing the front and extending into the opposing water mass (see for example Horne 1978; Woods *et al.* 1977; Gregg 1980). The case analysed by Gregg was in similar conditions to the one described here, in that no appreciable baroclinicity was observed, whereas the others occurred at fronts with a strong baroclinic signal. No comparable intrusions were seen in the data described here, although the deeper signals in the fixed ships' data (figures 3*a*, 5*b*, 5*e*) may be comparable and Van Aken (1981) has studied the interleaving in the deeper layers in the JASIN area. The kinematic model of cross-front intrusions presented by Woods *et al.* (1977) predicts the occurrence of inversions at the peaks of the meander displacement. In these data there does not seem to be a preference of inversions to be found at extreme lateral displacements in relative coordinates (inasmuch as these extremes are sampled).

Upwelling, as seen at the Malta front by Woods *et al.* (1977), is not observed in our data, but this is likely to be a consequence of the lack of strong baroclinicity at this front. The shapes of some isotherms, for example 12.2 °C in figure 4*a* are indicative of vertical motion at the front, resulting in cooler, denser water reaching the surface. In section 131N, for instance, the surface temperature (as measured by a near-surface device towed at nominal depth of 2 m; Pollard, this symposium) drops 0.1 K in a distance of about 100 m and then rises at a fairly

Downloaded from rsta.royalsocietypublishing.org

steady rate of about 0.11 K km^{-1} through 0.34 K. The drop in surface temperature was found at each crossing of the front although the surface temperature gradients were variable. The surface position of the front was thus marked by a braid of colder, denser water, which was located 0.9 ± 0.5 km (mean and standard deviation of 19 clear cases) to the east of the thermoclinicity maximum at the $\sigma_T = 26.70$ kg m^{-3} isopycnal. Since the thermohaline front sloped upwards towards the west, the cold surface water was well displaced from the position of the shallowest identifiable position of the thermoclinicity maximum (see figures 4*a*, *c*).

The assumption that Taylor's hypothesis holds over the period of the survey, so that the data could be plotted in relative coordinates, was made without any *a priori* justification. The results of numerical modelling of frontal instabilities (MacVean 1980) do not necessarily support this assumption, in that the growth rate of the fastest-growing instability on a front similar to the model front described above is 0.03 h^{-1} (i.e. the energy of the instability is doubled in about 31 h). The wavelength of this instability is about 8 km, which is reasonably close to the length scale of the observed meanders of 12 km. Another estimate of frontal meander scales is 9 km (I. Orlanski, cited in Woods *et al.* (1977) as private communication). Both of these are applicable to fronts with stronger baroclinicity than that observed here. If the observed meander is an unstable wave as modelled by MacVean, then it must propagate along the front. The phase speed of MacVean's most unstable wave is 20 cm s^{-1} (0.76 km h^{-1}), which compares with the advection speed of the front through the array. Obviously the situation is complex and requires further research.

5. Conclusions

With data from the Second Multiship Experiment of JASIN 1978, a detailed examination of the three-dimensional structure of an upper ocean thermohaline front has been possible.

The front is embedded in a larger-scale (order 100 km) anticyclonic eddy, which has distorted the background meridional temperature and salinity gradients, so that cool, less saline water lies to the east. The changes in the T, S properties across the front become negligible at $\sigma_T = 27.15$ kg m^{-3}, with thermohaline variability increasing again below. The presentation here concentrates on the structure above this level.

By using currents measured at the H2 mooring it has been possible to present the data in coordinates relative to the water, which was advected through the array of ships and buoys at about 0.75 km h^{-1}. This resulted in an advection of about 30 km in the along-front direction through the series of Sea-Soar sections. The main findings can be summarized as follows:

1. The thermoclinicity at the front was compressed into a very narrow band (sometimes less than 0.5 km wide), which became wider with depth as the inclination of the locus of maximum thermoclinicity increased. This is in accordance with the numerical results of MacVean & Woods (1980) who model frontogenesis in a current convergence acting on a weak baroclinic and thermoclinic zone.

2. The observed level of internal wave energy was too high for a change in the mixed-layer depth or baroclinicity on the scales of the observations (5 km) to be detected. Modulation of static stability was detected across the front.

3. Upwelling of cold water at the front led to the presence of a band of cool, dense water at the sea surface. This lay over the cold side of the front, about 1 km to the east of the thermoclinicity maximum at $\sigma_T = 26.70$ kg m^{-3}.

Downloaded from rsta.royalsocietypublishing.org

4. A modulation of thermoclinicity along the front was clearly seen with the frequent appearance of inversions, although these were less extensive than the cross-front intrusions reported elsewhere.

5. It has been possible to discount measured shears as being the source of meanders of the front, which are revealed in the relative coordinate system. The length scale of the meanders was 12 or 25 km, compared with 8 km predicted by a numerical model. The model, however, is of a front with stronger baroclinicity than that observed.

This complex data set could not have been collected without the whole-hearted cooperation of the masters and crews of the vessels involved, all of whom deserve thanks. The assistance of Margaret Saunders (IOS) and Stefan Hesse (IfM) in the initial processing of the data is gratefully acknowledged. Research funds from the Deutsche Forschungsgemeinschaft made possible the participation in JASIN of the German research ships, and supported some of us (M.K., A.H., and P.J.M.) while working on these data.

References

Baumann, R. J., Paulson, C. A. & Wagner, U. 1980 Towed thermistor chain observations in JASIN. Report 80-14, School of Oceanography, Oregon State University.

Baker, D. J. 1981 Ocean instruments and experiment design. In *Evolution of physical oceanography* (ed. B. A. Warren & C. Wunsch), pp. 396–433. Cambridge, Massachusetts, London: MIT Press.

Brown, N. L. 1974 A precision CTD microprofiler. IEEE International Conference on engineering in the ocean environment record, *Ocean 1974*, vol. 2, 270–278.

Defant, A. 1961 *Physical Oceanography*, vol. 1. Oxford, New York: Pergamon Press.

Dessureault, J. G. 1976 'Batfish'. A depth controllable towed body for collecting oceanographic data. *Ocean Engng.* **3**, 99–111.

Gregg, M. C. 1980 The three dimensional mapping of a small thermohaline intrusion. *J. phys. Oceanogr.* **10** 1468–1492.

Halpern, D. 1979 H2 current and temperature measurements. Data report, NOAA Pacific Marine Environmental Laboratory, Seattle, U.S.A.

Horch, A., Minnett, P. J. & Woods, J. D. 1982 CTD measurements made from FS *Poseidon* during JASIN 1978: a data report. Berichte aus dem Institut für Meereskunde, Kiel, no. 97.

Horne, E. P. W. 1978 Interleaving at the subsurface front in the slope water off Nova Scotia. *J. geophys. Res.* **83**, 3659–3671.

Kroebel, W. 1973 Die Kieler Multimeeressonde. *MeteorForsch Ergebn.* A**12**, 53–57.

Legekis, R. 1978 A survey of world-wide sea surface temperature fronts detected by environmental satellites. *J. geophys. Res.* **83**, 4501–4522.

MacVean, M. K. 1980 Report on the project 'Theoretische Untersuchung von ozeanischen Fronten'. Institut für Meereskunde, Kiel.

MacVean, M. K. & Woods, J. D. 1980 Redistribution of scalars during upper ocean frontogenesis: a numerical model. *Q. Jl R. met. Soc.* **106**, 293–311.

Minnett, P. J. 1978 Mesoscale variability in the tropical thermocline during GATE. Ph.D. thesis, University of Southampton.

Oakey, N. S. 1982 Determination of the rate of dissipation of turbulent energy from simultaneous temperature and velocity shear microstructure measurements. *J. phys Oceanogr.* **12**, 256–271.

Pollard, R. T. 1980 Reduction of JASIN Batfish data. JASIN News. no. 17.

Pollard, R. T. 1982*a* Mesoscale (50–100 km) circulations revealed by inverse and classical analysis of the JASIN hydrographic data. *J. phys. Oceanogr.* (In the press.)

Pollard, R. T. 1982*b* Eddies and fronts in the JASIN area. JASIN News, no. 25.

Pollard, R. T. & Saunders, P. M. 1978 Air–sea interaction: the structure of the upper ocean during JASIN 1978. R.R.S. *Discovery* cruise 94, Cruise report no. 74, Institute of Oceanographic Sciences, Wormley.

Stern, M. E. 1975 *Ocean circulation physics.* New York, San Francisco, London: Academic Press.

Van Aken, H. 1981 The thermohaline fine structure in the North Rockall Trough. Doctorate thesis, State University of Utrecht.

Woods, J. D., Wiley, R. L. & Briscoe, M. G. 1977 Vertical circulation at fronts in the upper ocean. In *A voyage of Discovery* (ed. M. Angel), pp. 253–275. Oxford, New York: Pergamon Press.

Downloaded from rsta.royalsocietypublishing.org

Discussion

M. C. Gregg (*Applied Physics Laboratory, University of Washington, 1013 Northeast Fortieth Street, Seattle, Washington* 98105, *U.S.A.*). Dr Minnett described the results of applying the MacVean frontal model to some of the data obtained during JASIN. Could he outline the key assumptions of the model?

P. J. Minnett. MacVean & Woods (1980) describe the effect of a two-dimensional barotropic horizontal deformation field ($u = -\alpha x$, $v = \alpha y$) acting on existing weak horizontal gradients of density and temperature. The initial conditions and the deformation rate, α, of 10^{-5} s^{-1} are believed to be realistic representations of oceanic conditions. The along-front flow is assumed geostrophic and the effects of turbulent mixing are neglected as sub-critical Richardson numbers are not encountered until the front is well developed. This takes three to four days.

In addition to the aspects discussed in the above paper, the model also predicts a sharp change in the depth of a mixed layer overlying a pycnocline front.

J. D. Woods (*Institut für Meereskunde, Düsternbrooker Weg* 20, *D*-2300 *Kiel, F.R.G*). In response to the question from Professor Gregg about the MacVean–Woods model let me emphasize the key assumption made in the model, namely that the motion is adiabatic, so that particles conserve potential vorticity as they flow into the jet, and then along it. The relative vorticity associated with the horizontal shear at the jet is accompanied by a corresponding change in the spacing between the isopycnals. In the model the cyclonic shear at the jet is about equal to the planetary vorticity (f) after four days, doubling the spacing between the isopycnals near the surface. It has been shown in a later paper that the flow curvature associated with meanders of the kind observed in the JASIN front give additional relative vorticity of order f. In the GATE front (Woods *et al.* 1981) the spacing of isopycnals is dilated by up to six times the mean, at depths well below the influence of the mixed layer. The low latitude of the GATE experiment gave large dilation for modest relative vorticities. For the JASIN front (at high latitude) the observed dilation factor of five in the isopycnal spacing could only be achieved adiabatically by cyclonic relative vorticities much larger than those in the GATE front. That seems unlikely for a front that has weak baroclinicity (according to the interpretation of the JASIN data by Minnett *et al.*), though it is not dynamically impossible. But one has to remember that the JASIN data come from the weakly stable 'potential layer' lying between the mixed layer and the seasonal thermocline. During the Second Multiship Experiment the weather was calm, and the mixed layer did not descend through the potential layer to the top of the seasonal thermocline, even at night. So the water may have been conserving potential vorticity (to the limit set by solar heating) while the measurements were being made. But perhaps the large observed variations of isopycnic spacing were in part the result of the interaction between the vertical motion induced by relative vorticity changes and the diabatic processes in the mixed layer some days earlier when it was deeper.

Reference

Woods, J. D., Leach, H. & Minnett, P. J. 1981 The GATE Lagrangian Batfish Experiment. Berichte aus dem Institut für Meerskunde, Kiel, no. 89.

PHILOSOPHICAL TRANSACTIONS OF THE ROYAL SOCIETY A MATHEMATICAL, PHYSICAL & ENGINEERING SCIENCES

PHILOSOPHICAL TRANSACTIONS OF THE ROYAL SOCIETY A MATHEMATICAL, PHYSICAL & ENGINEERING SCIENCES

Downloaded from rsta.royalsocietypublishing.org

S. A. Thorpe (*Institute of Oceanographic Sciences, Brook Road, Wormley, Godalming, Surrey GU8 5UB, U.K.*). The observations of thermoclinicity in the front were compared with a theoretical model. How is the vertical scale within which the thermoclinicity turns near the surface related to the external forcing in the model, and is a similar scale predicted by observation?

P. J. Minnett. The length scale of the turning of the thermoclinicity is not related to a vertical length scale in the forcing field in the model as this is barotropic. Any possible dependence of the thermoclinicity-turning length scale on the size of the imposed deformation rate is not investigated in MacVean & Woods (1980). They do, however, report that the shape of the thermoclinicity structure of the developed front depends on the initial fields of density and temperature. Thus the thermoclinicity-turning length is most likely to be determined by the background conditions on which the deformation field acts rather than by the deformation field itself.

M. G. Briscoe (*Woods Hole Oceanographic Institution, Water Street, Woods Hole, Massachusetts* 02543, *U.S.A.*). Is it possible to interpret the diagram showing north–south extent of the front, which was based on 40 hours of data, as showing an older, more developed front in the northern parts? (This seems possible since 40 hours is a substantial fraction of the MacVean–Woods frontogenesis model.) If so, then perhaps it is not surprising that the frontal overturning is predominant in the northern part of the front.

P. J. Minnett. The true nature of the observations undoubtedly consists of elements of both temporal and spatial changes, and, in principle, this alternative interpretation of figure 7 may be correct. However, for the following reasons, I believe the interpretation given in the paper to be more valid.

Firstly, the similarity of some sections closely spaced in relative coordinates but separated in time (e.g. 137N and 141S) lends weight to the interpretation that the signal is predominantly spatial. Secondly, the model predicts that, throughout the period of frontogenesis, thermoclinicity becomes more concentrated at all depths. Examination of the isotherms on the $\sigma_T = 26.70$ kg m^{-3} isopycnal (figure 8*a*) shows that increased thermoclinicity in later sections was not observed.

As mentioned in the discussion, the assumption that Taylor's hypothesis holds during the period of the observations cannot be satisfactorily confirmed, but I believe the most likely source of rapid changes is instabilities on the front rather than frontogenesis. This is borne out by the meander-like pattern in figures 7 and 8*a*. Perhaps I should stress that the data were not taken in a Lagrangian frame (i.e. following a particular piece of water as it was advected by the current), in which case a predominantly temporal signal might have been expected.

J. D. Woods (*Institut für Meereskunde, Düsternbrooker Weg* 20, *D*-2300 *Kiel, F.R.G.*). I do not agree with Dr Briscoe's suggestion that spatial changes might be interpreted as temporal variation of the front during frontogenesis. Firstly, it is unlikely that one happens to survey a front during the early stage of frontogenesis, which lasts for only a few days, whereas the front persists for the lifetime of many weeks of the eddy deformation field that created it. Secondly, the existence of large-amplitude meanders shows that frontogenesis has been completed; the meanders grow *after* the baroclinicity has been sharpened by frontogenesis.

PHILOSOPHICAL TRANSACTIONS OF THE ROYAL SOCIETY A MATHEMATICAL, PHYSICAL & ENGINEERING SCIENCES
PHILOSOPHICAL TRANSACTIONS OF THE ROYAL SOCIETY A MATHEMATICAL, PHYSICAL & ENGINEERING SCIENCES